3-2005

Design and Simulation of a Permanent-Magnet Electromagnetic Aircraft Launcher

Dean Patterson

Antonello Monti
University of South Carolina - Columbia, monti@engr.sc.edu

Charles W. Brice
University of South Carolina - Columbia, brice@cec.sc.edu

Roger A. Dougal
University of South Carolina - Columbia, dougal@engr.sc.edu

Robert O. Pettus

See next page for additional authors

Author(s)

Dean Patterson, Antonello Monti, Charles W. Brice, Roger A. Dougal, Robert O. Pettus, Srinivas Dhulipala, Dilip Chandra Kovuri, and Tiziana Bertoncelli

Design and Simulation of a Permanent-Magnet Electromagnetic Aircraft Launcher

Dean Patterson, *Senior Member, IEEE*, Antonello Monti, *Senior Member, IEEE*,
Charles W. Brice, *Senior Member, IEEE*, Roger A. Dougal, *Senior Member, IEEE*, Robert O. Pettus,
Srinivas Dhulipala, Dilip Chandra Kovuri, and Tiziana Bertoncelli

Abstract—This paper describes the basic design, refinement, and verification using finite-element analysis, and operational simulation using the Virtual Test Bed, of a linear machine for an electromagnetic aircraft launcher, for the aircraft carrier of the future. Choices of basic machine format and procedures for determining basic dimensions are presented. A detailed design for a permanent-magnet version is presented, and wound-field coil and induction machine versions are briefly discussed. The long armature–short field geometry is justified, and in particular the impact of this geometry on the scale of the power electronic drive system is examined.

Index Terms—Aircraft launcher, linear machine, linear permanent-magnet (PM) synchronous machine, PM machine, power electronic drive, system simulation, track sectioning.

I. INTRODUCTION

A. The Project

MODERN ship designs are increasingly moving toward the use of electricity to distribute, control, and deliver energy for the multiplicity of on-board needs. This trend has already resulted in large direct-drive electric machines for traction in commercial shipping. In some significant cases, including traction, adoption in military applications is rather slower, because of the comparatively low achievable power, energy, and torque per unit volume and per unit mass, of electromechanical energy conversion systems.

However, the benefits of controllability, robustness, reliability, damage management, operational availability, reduced manning, etc., are undeniable. While all actuation systems are under continuous investigation, there is a high level of interest in determining the feasibility of an electromagnetic aircraft launcher (EMAL) for aircraft carriers [1], [2].

Studies are being carried out at the University of South Carolina (USC), Columbia, to evaluate alternative design concepts and to determine their feasibility and comparative strengths [3]. Simulation uses the Virtual Test Bed (VTB), a new environment for simulation and virtual prototyping of power electronic systems that includes not only simulation of system dynamics, but also solid modeling of the system and visualization of the system dynamics [4].

An EMAL also represents a challenging test case for VTB itself. Models of the different parts of the systems are being built up from the specifications and the characteristics of a typical system, and from engineering design principles.

B. The Challenge

The design of an EMAL has many intriguing challenges. The likely specifications and technical features include the following:

- *maximum velocity*—100 m/s;
- *power stroke*—100 m;
- *braking distance, moving member*—10 m;
- *maximum energy*—120 MJ;
- *maximum thrust*—1.3 MN;
- *minimum time between launchings*—∼ 50 s.

Acceleration to the maximum velocity requires a 2-s stroke, at a constant acceleration of 5 g. The joule limit implies that this aircraft would have to have a mass of less than 24 t. Heavier aircraft can, of course, be launched to lower terminal velocities.

While the overall system design must include storage, power electronics, and control system design, this paper will concentrate on the electric machine design, and introduce some of the power electronics and control issues.

II. LINEAR MACHINE DESIGN

A. Background

A substantial body of research exists on large linear motors; however, the majority of these are induction machines, and by far the largest number of these are what are known as short primary–long secondary machines. We will also use the terminology short armature–long field for this geometry, a little more apt for noninduction machines. Significant issues in design of these machines are the study of both edge effects and end effects [5]–[10].

D. Patterson is with the Electrical Engineering Department, University of Nebraska, Lincoln, NE 68588-0511 USA (e-mail: patterson@ieee.org).
A. Monti, C. W. Brice, R. A. Dougal, and R. A. Pettus are with the Department of Electrical Engineering, University of South Carolina, Columbia, SC 29208 USA (e-mail: monti@engr.sc.edu; brice@engr.sc.edu; dougal@engr.sc.edu; pettus@engr.sc.edu).
S. Dhulipala was with the Department of Electrical Engineering, University of South Carolina, Columbia, SC 29208 USA. He is now with Orion Systems Integrators, Edison, NJ 08820 USA (e-mail: srinivasd@gmail.com).
D. C. Kovuri was with the Department of Electrical Engineering, University of South Carolina, Columbia, SC 29208 USA. He is now with BNP paribas, New York, NY 10019 USA.
T. Bertoncelli is with the Dipartimento di Elettrotecnica, Politecnico di Milano, 20133 Milan, Italy (e-mail: tiziana.bertoncelli@polimi.it).
Digital Object Identifier 10.1109/TIA.2005.844404

Fig. 1.   Electromagnetic shear stress definition.

Fig. 2.   Inverted U shuttle.
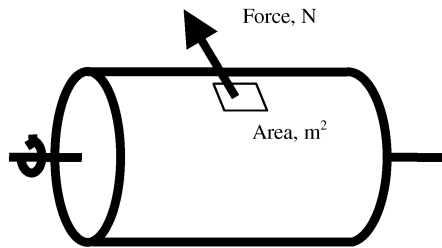

Fig. 3.   Blade shuttle.

A common application of short primary–long secondary machines is for traction in electric trains, where the energy is delivered to the train via a catenary or third-rail system, and applied to an on-board armature or primary. The secondary, or field, member is some form of complete track-length reaction rail. The Westinghouse "Electropult," developed during World War II, is an aircraft-launching linear induction machine of this form [11].

The issue of the transfer of >120 MJ in 2 s to a moving member (referred to hereinafter as the shuttle) either through sliding contacts or some form of moving harness is daunting. The "Electropult" referred to above used sliding contacts; however, the thrust required for this EMAL project is about 20 times greater than that delivered by the Electropult. A historical description of the Electropult says, "... the operational costs were so high that in spite of the encouraging performance, steam catapults held the field".[1] The simplicity of the dc motor driven flywheel and the linear induction machine with a flat "squirrel-cage" stator lead one to the conclusion that the operational costs must have been particularly associated with the sliding contacts. The need to decelerate the shuttle also makes minimization of shuttle mass a strong design constraint. These factors, together with the limited length of travel, have led to the study of long primary–short secondary, or long armature–short field machines.

B. Basic Machine Sizing

Initial sizing of any machine is often done by considering "electromagnetic shear stress," as defined in Fig. 1.

Miller quotes numbers for typical machines as being between 0.7–2 kN/m^2 for fractional horsepower induction machines ranging up to between 70–100 kN/m^2 for very large liquid-cooled machines such as turbine generators, adding that peak rating may exceed these values by a factor of 2–3 [12].

The Electropult, which can be considered as an induction machine with variable resistance "rotor," operated at a stress of a little greater than 50 kN/m^2. This is reasonable for a machine which was highly inefficient, being driven with a constant 60 Hz, and thus spending most of its operational time at a slip of greater than 50%.

C. Shuttle Mass

It turns out that the issue of stopping the moving member electrically in the minimum distance specified is a particularly
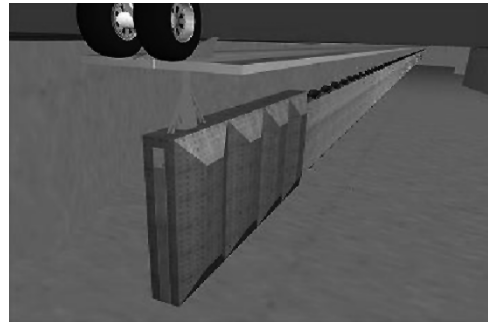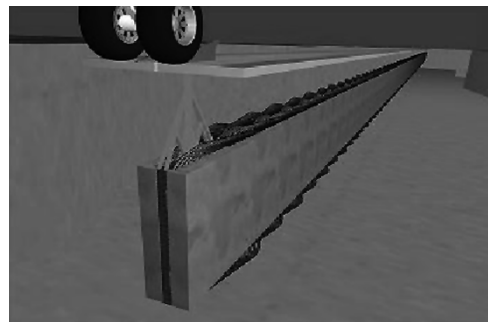
significant constraint on the design. Of course solutions are possible with shorter acceleration distances and longer braking distances, however, shortening the acceleration distance must necessarily put greater strain on the airframe, and this is a very significant problem, which should be addressed if at all possible [13]. The maximum possible mass that can be decelerated from 100 m/s in 10 m by applying the reversed electrical thrust of −1.3 MN, assuming that the deceleration section is simply an extension of the acceleration section, but driven for reverse thrust, is 2.6 t. This mass has a kinetic energy at 100 m/s of 13 MJ, one-tenth of the maximum launching energy. Clearly, we would want to recover this if possible, and the issue of a friction or water brake (as is used in the steam catapult) to manage 13 MJ regularly is not simple, although a passive "one-time use" emergency system must be in place if the normal braking method is electrical active.

The permanent-magnet (PM) design presented below has a shuttle mass of 2.2 t maximum, and operates at 220 kN/m^2. At the end of the paper in Section V specific engineering challenges in a wound-field and an induction version of this launcher are discussed.

D. Basic Machine Format

In order to achieve the surface area determined by achievable stress figures, two geometries were considered, the "inverted U" and the "blade," as shown in Figs. 2 and 3.

While for the inverted U the overall machine will be lighter, the mass of the shuttle must include material for completing the magnetic circuit. The amount of material is strongly dependent on the pole pitch; however, at reasonable values of pole pitch the mass of an iron return path, as required for an induction version, is high, computing to ∼1 t. To this must be added the support

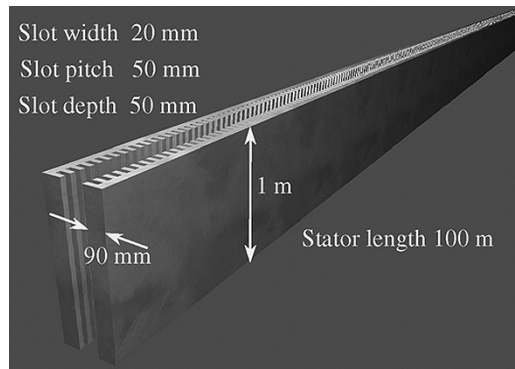[1]http://historia.et.tudelft.nl/pub/art/machines.php3#III3

Fig. 4.   Stator dimensions.

structure, and the PMs in the case of a PM machine. An option not yet considered in detail would be the use of PM Halbach arrays on each side [14]. However, preliminary calculations still indicate that the 2.6-t limit will be difficult to achieve.

In contrast, the blade structure allows the lightest possible shuttle, and a total mass of the two-sided stator which is well within the design goal mass. This two-sided stator also has very good thermal paths.

Of course, in practical implementation, the structure will use at least two separate blades or inverted U's to allow for the mechanical support structure and the requisite bearings, for much the same reasons that the steam catapult uses two cylinders and two pistons. However, a single-blade structure is discussed in this paper, on the understanding that at least in electrical and magnetic terms, multibladed systems are simply a mechanical transformation of, and can be derived from, the single-bladed system.

1) Pole Pitch: Pole pitch is a very significant determinant of machine performance. Short pole pitches lead to higher efficiencies (less end-turn length), thinner back iron on the stator sections (important for total mass), and are usual in high torque/force machines of large size. Limitations on indefinite reduction of the pole pitch have to do with the fundamental frequency of the drive power, which is also the frequency of flux reversal in parts of the magnetic structure, resulting in core loss, and fringing effects between adjacent poles. These fringing effects are related to the minimum achievable air gap. A pole pitch of 150 mm was chosen as a compromise, resulting in a maximum frequency in the steel of 333 Hz which is easily managed by standard laminated steel, and a low overall mass. It will be shown later in Section IV-B.2 that there are also substantial penalties in terms of the power electronics drive which would result from shortening the pole pitch further.

2) Stator and Slot Dimensions: It has been shown that, at least for surface PM machines, eddy-current loss in the stator teeth is proportional to the number of slots per pole per phase [15]. At the minimum one slot per pole per phase, with a traditional lap winding, a stator as shown in Fig. 4 was dimensioned to suit the above chosen pole pitch, and the necessary surface area common to the shuttle and the stators.

The steel of the stator has a total mass of 100 t. The steam catapult this system is to replace has a total mass of 486 t, so this stator should result in a total machine with substantial mass savings. The thermal mass of the 100-t structure is such that an

energy dump of 6 MJ, which results from a single launching at the worst load case in the PM design presented here, will result in <0.2 °C temperature rise per launch. Thus, active cooling will not be necessary in any part of the PM machine.

As will be seen below, the inductance of the winding is a primary determinant of the complexity of the power electronic drive system, so that the stator is designed with open slots to minimize winding inductance. The stator winding scheme, using the traditional three phases, which are not obligatory but give a good starting position for a first design, is as summarized in Fig. 5.

E. Driving the Armature

Using the PM machine stress of 220 kN/m^2 introduced above yields a shuttle length of 3 m. We begin by assuming a standard six-step servo drive, a pole pitch of 150 mm, a likely achievable flux density in the air gap of 0.9 T, and a total thrust of 1.3 MN. A slot current of 18 kA results.

If this is in a single conductor in the slot, of size $15 * 40$ mm (60% fill factor), a current density of 30 A/mm^2 results, yielding an estimated total copper loss of 2 MW for the complete launcher. Since the machine rating is 60 MW, copper losses represent only some 4% of the input power.

The more important issue is that, confirmed by finite-element analysis (FEA), the inductance of the single conductor in the slot is ~2.6 μH/meter. Of course, the single conductor can be divided, reducing the individual conductor current and the switch current, using more than one turn for the winding, without affecting the copper loss (providing the same fill factor results). However, the inductance goes up as N^2, where N is the number of turns.

Even at one turn, the inductance of a single phase 200 meters in length for both sides, pole pitch 150 mm, without considering end turns (where the inductance is much lower, not being in iron), computes to 3.5 mH. In order to commutate from +18 kA to −18 kA at a 333-Hz rate, a supply voltage of 250 kV would be required. Clearly, driving the track in sections is the only feasible option.

F. Simulation

The discussion so far has indicated the very large range of possibilities that need to be compared and considered when conceiving of a system of this complexity. Most commonly, promising research directions are deduced from data taken from existing operating systems. Without operational systems to guide research, recourse must be made to very powerful cross-disciplinary system simulators.

1) VTB: VTB is an ideal tool to explore the many possible variants for an EMAL, and to facilitate convergence on optimal solutions. The project is enabling experience in machine design and simulation to be applied to a very detailed study of this very large pulsed-power application, focusing on a range of important criteria. These include total system mass, total system volume, thermal management, reliability, robustness, survivability via redundancy, and also acoustic, magnetic, and electromagnetic signatures. These considerations are in addition to very real challenges in the many control loops in an EMAL, up to and including totally sensorless control.
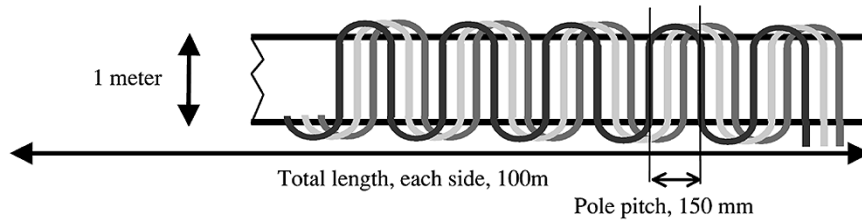
Fig. 5. Three-phase one-slot-per-pole-per-phase stator winding (armature) structure.
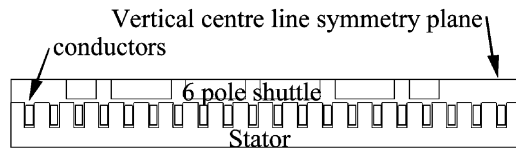

Fig. 6. Geometry used for FEA.

III. DETAILED PM MACHINE DESIGN

At the pole pitch of 150 mm discussed above, a 3-m shuttle would involve some 20 poles of Neodymium Iron Boron (NdFeB) magnet material, supported in a composite structure. The magnet thickness is determined by two things:

1) minimum feasible air gap and the design requirement for near to 0.9T in that air gap
2) requirement that the slot current of 18 kA not demagnetize the PM material.

The design analyzed uses an 8-mm air gap on each side, and a total magnet thickness of 80 mm. Using 120° magnet widths, the total magnet mass for the shuttle computes to 1184 kg. At 100 m/s, and increasing the mass by 40% for the supporting composite structure, the shuttle has a kinetic energy of 8.3 MJ. Using the same winding scheme as for launching, producing a reverse thrust of 1.3 MN, this shuttle can be stopped electrically, with full energy recovery, in 6.4 m, well inside the allowed distance of 10 m. The stopping time is 127 ms, and the deceleration is ∼80 g, so the support structure must be designed to manage this deceleration for the material, as well as the transference of the thrust to the airframe during acceleration.

A. FEA

Two-dimensional (2-D) FEA has been used to verify certain aspects of the design, and to make refinements. The shuttle with 120° (100 mm) magnet widths, and 20 poles of alternating polarity, begins and ends with a half-width magnet. For simplicity in modeling, the analyzed shuttle had a length of five pole pitches. The shuttle begins and ends with a half-width pole, for a total of six magnetic poles, as shown in Fig. 6. Note that only half of the geometry is entered, invoking symmetry around a center line. Thus, the drawing is of a top view of one side of a short section of the complete machine.

1) Demagnetization and Saturation: This model was analyzed for the vertical component of B in the magnets with 18 kA in the conductors, which is never below 0.4 T in the direction of magnetization so that demagnetization is not an issue. The magnet thickness used here is necessary only to keep a very high flux density in the chosen air gap. Clearly, other designs could use a higher electric loading and a lower flux density with
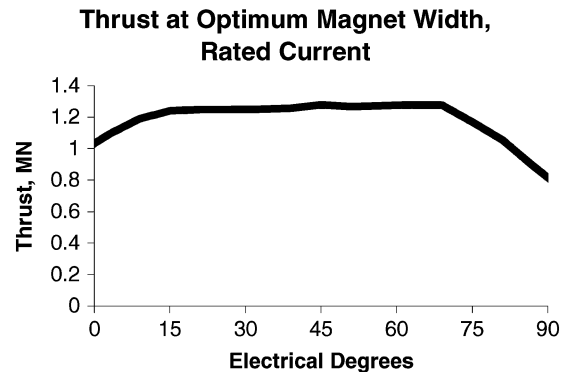

Fig. 7. Thrust determined by FEA for constant current in two phases, as a function of shuttle position in electrical degrees.

less magnetic material and less shuttle mass; however, those designs would require higher di/dt's in the windings. As we shall see, this impinges seriously on the overall operation. The FEA model was also used to verify that despite quite substantial saturation in the steel the design thrust is achievable at the design current.

2) Thrust Ripple: Rectangular magnets and open slots as shown above are capable of developing very substantial cogging forces which can add to any thrust ripple when the stator is driven. Thrust ripple needs to be minimized to avoid unwanted stress on the airframe. While thrust ripple can be controlled by current control, it is also common practice in design to vary the magnet width to control the cogging force. The option to vary the magnet width to minimize not the cogging force but the thrust ripple with constant current in the windings was exercised with surprisingly effective results.

Fig. 7 shows the thrust as a function of position with two windings energized with constant current, as is usual with simple six-step switching. At the optimal width, the thrust is surprisingly constant over the necessary 60 electrical degrees. Since each phase will be independently controlled, handover at the edges of each step can be managed to provide a smooth transition from one phase pair to the next.

B. Power Electronics

While the machine design turns out to be surprisingly simple, the power electronics design, particularly with the long armature–short field geometry, is challenging, and very much dependent on the ratings of available switches. As discussed above in Section II-E, the track must be sectioned into drivable lengths. In order to provide a high level of control, to provide high levels of redundancy, and to provide the option to use other than three

phases, it was decided to drive each separate phase winding in each section independently, with its own H-bridge.

1) Typical Devices: A very promising device, and one for which USC has been developing models, is the integrated gate commutated thyristor (IGCT). One of the principal models developed is for a device with a rating of 4 kV and 2.4 kA. Two of these in parallel can be used as a switch element to make an H-bridge with 4-kV 4.8-kA ratings. This configuration has been adopted for the early simulations. In order to manage 18 kA in each slot, it was decided to use four independent turns in each phase, each with its own H-bridge, so that in any section of the track $3*4 = 12$ H-bridges are required.

2) Sectioning the Track: At every point along the 100-m track a maximum drivable inductance can be calculated, based on the maximum possible velocity at that point. For example, at the end of the track the maximum velocity is 100 m/s. The ΔI is from $-$ to $+4.8$ kA, or 9 kA, the ΔT is, from the velocity and the pole pitch $= 0.5$ ms, the E manageable by the bridge is 4 kV, resulting in an $L_{\mathrm{max,100\ meters}}$ of 0.22 mH.

This inductance results from both sides of 5 m of track for a single turn of a single phase. This winding starts at 100 m on, for example, the left-hand side of the track, goes back to 95 m, crosses underneath, and then returns from the 95-m point to the end at 100 m. Thus, the final section of the track to be driven, given the available switches, can be only 5 m in length.

Since a winding begins and ends at the same place, the cables from the power electronic drive to that section can be configured for very low inductance, as for example, in parallel bus bars.

An expression for the drivable length ΔX at any distance x along the track can be derived by following the procedure above to compute a maximum drivable inductance at any point x, determined by the maximum possible velocity at that point, and then introducing L_s, the inductance/meter in the slot, as

$$\Delta X = \frac{V_b p_p^2}{6 L_s D_s \Delta I \sqrt{2ax}} \tag{1}$$

where V_b is the available bus voltage, p_p is the pole pitch, L_s is the inductance/meter in the slot, D_s is the length of the slot, ΔI is the current change, a is the acceleration, and x is the distance along the track. This formula has been derived for six-step switching, commutating the current by ΔI in 1/6 of a period. The back electromotive force (EMF) does not appear on the assumption that for a trapezoidal back EMF, the average back EMF over this time interval is zero.

Note particularly the significance of pole pitch, so that track sectioning can be dramatically reduced by increasing the pole pitch.

The equation above is for a fixed physical design, and is of the form

$$\Delta X_n = kx^{-1/2}$$

which for the machine constants of this design, is graphed in Fig. 8. Applying this sectioning to the design results in 12 sections, increasing in length from 5 to 15 m for the initial section.

No more than two sections are ever activated at any one time, since the shuttle of 3-m length is shorter than any section. Therefore, in operation, Section 1 of the track is activated, and the

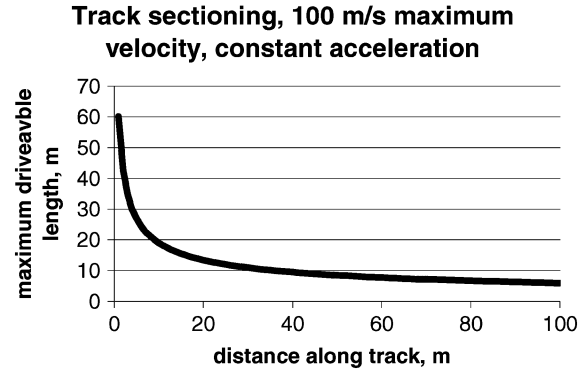**Track sectioning, 100 m/s maximum velocity, constant acceleration**

Fig. 8. Track section length as a function of position.

shuttle begins to move. As the leading edge of the shuttle arrives at the start of Section 2, Section 2 is activated as well, and then as the trailing edge of the shuttle leaves Section 1, Section 1 is deactivated. The H-bridge set that was driving Section 1 can be disconnected from Section 1, and connected to Section 3 in readiness for the arrival of the leading edge of the shuttle at the start of Section 3.

3) Power Electronics Switching Matrix: Thus, a workable switching matrix involves two sets of 12 H-bridges. Connection of each bridge in a set to one of six sections (one set drives section numbers 1, 3, 5, 7, 9, and 11, and the other set drives the even numbers) can be done using back-to-back thyristors. These thyristors would be continuously triggered when required, and will switch off when the current decays to zero, when the H-bridge switches are no longer driven. There is adequate time in all cases for this to happen. Figs. 9 and 10 show the overall matrix structure, and the H-bridge–thyristor connections, respectively.

IV. VTB SIMULATION

The authors are currently refining models for all of the individual system components. The current status of the simulation is reported below. A simulation-driven animation of the three–dimensional (3-D) system showing the obtainable performance has been produced.

A. Machine Modeling

Work began with a standard d–q model for a generic PM machine [16]. This has been adapted, replicating in the modeling structure the modularity of the EMAL motor. The model architecture has two separate parts, the stator winding models (one for each section), and the shuttle model. The system is designed so that any set of independent stator section models can be connected to a single shuttle.

The stator model simulates the current in each single winding in a section, and it defines the force contribution of that section to the overall system force. The superposition theorem is applied in the shuttle model to sum the force generated by each winding in each section and then to solve the mechanical equations for speed and position. This information is sent back to the stator sections in order to evaluate the back EMF.

The equivalent circuit of each stator section model is shown in Fig. 11. Each winding is represented by its equivalent circuit.
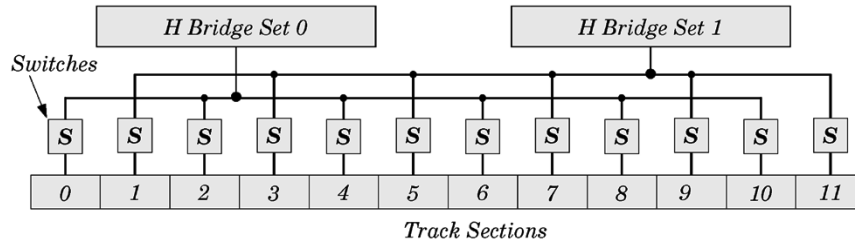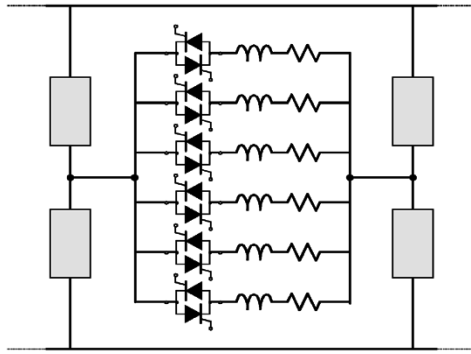
Fig. 9. Overall switching matrix.

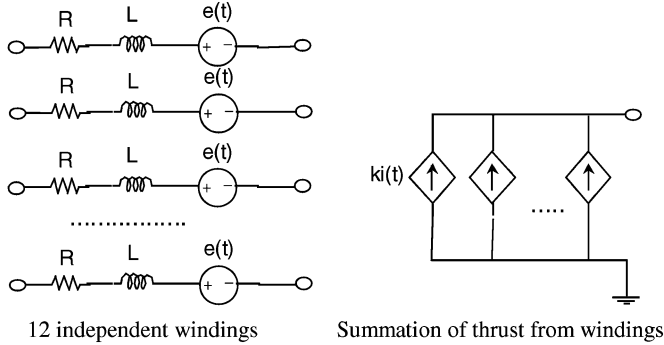Fig. 10. H-bridge—thyristor-winding connections.

Fig. 11. Equivalent circuit of the stator model.

Since the design suggests four turns for each phase, the model has the 12 independent circuits for the three phases in any single section.

The evaluation of the electromotive force and the mechanical force coefficient is based on the mechanical position and velocity. First of all, a check is performed to determine if the shuttle is over the section, so that the effect of the PM is present, and then a check of the position within the section determines the specific values.

In particular, for the evaluation of the thrust, the following equation is adopted:

$$T = K_p n \sum_{k,j} \left(\frac{\partial \psi}{\partial x} \right)_{k,j} i_{k,j}$$

where

- $i_{k,j}$ is the current in the jth winding of the kth phase;
- $(\partial \psi / \partial x)_{k,j}$ is the derivative of the flux of the PM with respect to distance, as seen by the jth winding of the kth phase;
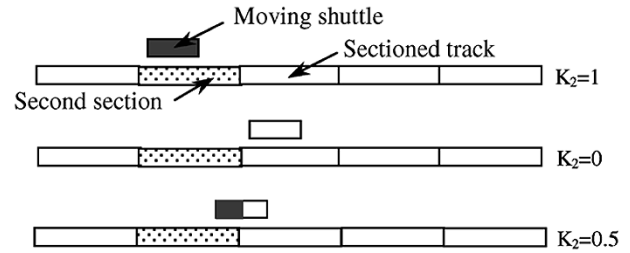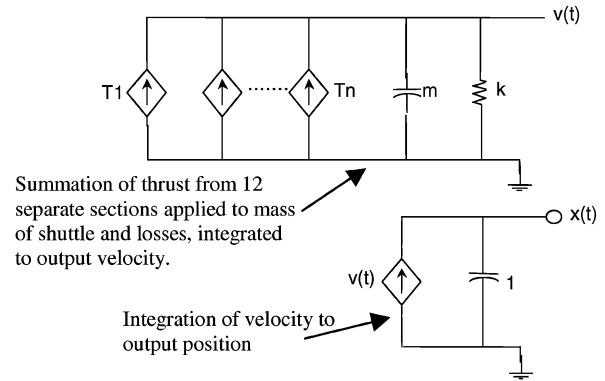- n is the number of pole pairs;

Fig. 12. Definition of coefficient K_2 (for the second section).

Fig. 13. Equivalent circuit of the moving part.

- K_p is a coefficient introduced to manage the amount of overlap of the shuttle and stator section p; if the shuttle is completely over a section p this coefficient will be unity; this is illustrated in Fig. 12 for $p = 2$.

The shuttle is modeled through the equivalent circuit shown in Fig. 13.

This circuit has two separate sections. The velocity is calculated by summing the forces from all 12 sections, subtracting the losses, and having this resultant thrust acting on the mass of the shuttle represented by a capacitor to provide the integration. The position calculation is then obtained as an integration of the velocity.

A set of tests was performed to validate the modeling approach. The VTB schematic for the first test is given in Fig. 14.

The pins on the bottom are the electrical terminals, while those on the left are for the mechanical interface. In this case the speed and position are fixed to zero (the two pins on top are grounded—equivalent to a locked-rotor test), while a square-wave voltage feeds one winding. This test verifies the correctness of the electrical subsystem and a classical R–L transient is the computed result as seen in Fig. 15.
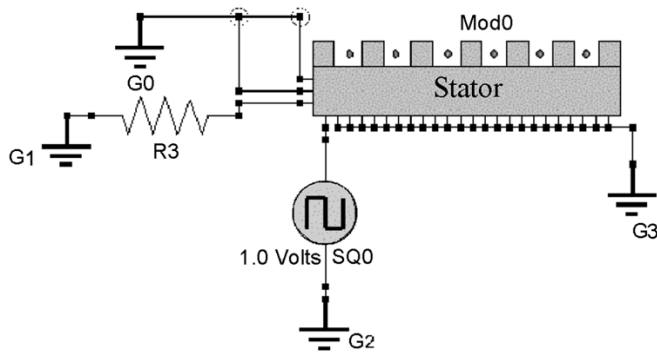
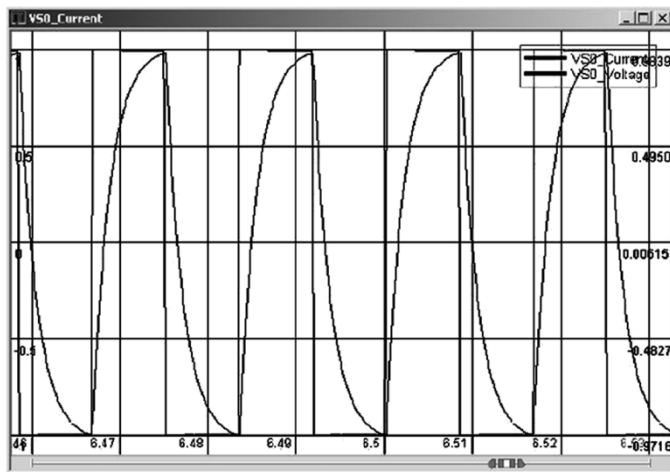Fig. 14.   VTB schematic for first simulation test.

Fig. 15.   Results of the first test.

A second test, with the VTB schematic as in Fig. 16, validated the mechanical model. In this case we have three stator section models and one shuttle model. A constant velocity is applied to the shuttle and then we measure the voltage across the open-circuited stator electrical windings.

In this case we see in Fig. 17 the classical trapezoidal waveform that appears only for those sections that are under the shuttle. We also see the amplitude being related to overlap, via the factor *Kp*, and we see that successive sections are of different length.

B. Converter Modeling

All the switching alternatives are considered. A completely separate drive circuit for each coil is seen as the best solution, although the issue of current control of the magnetically coupled coils in the same slot has yet to be addressed. Averaged models of power electronic building block (PEBB)-like converters have been used to speed up the simulation, but switched versions can also be used.

In the first simulation a single H-bridge configuration for each phase was adopted: This means that a single converter was connected to four different windings in parallel. This is reasonable since we are using ideal switch models at this stage.

C. Control Modeling

The controller was modeled by using the VTB-Simulink interface. The controller is designed to fulfill the following requirements.

- Each independent coil is fired by shuttle position sensors located along the stator,
- Preset current (thrust) levels in each coil are known,
- Open-loop operation is possible if communication fails or is damaged,
- If communication exists, each coil thrust is adjusted as it is firing, so as to ensure adherence to the required thrust/velocity profile.

The control algorithms are designed in Simulink, tested interactively, and finally compiled for better simulation performance.

The modular structure of the motor requires a hierarchical structure for the thrust control. Only one thrust control, or System Manager is used, and as many current controllers or Hardware Managers as the number of H-bridges. The System Manager decides, from shuttle position information, in which sections to control current.

V. SIGNIFICANT ENGINEERING CHALLENGES IN ALTERNATIVE MACHINE TYPES

While the original project brief sought a comparative examination of machine types, including wound-field and induction versions of the launcher, the results have indicated a very clear advantage for the PM version. The two sections below summarize the reasons why those two alternative versions were considered to have significant engineering challenges not associated with the PM version.

A. Wound-Field Machine

An FEA model was constructed with the stator dimensions as for the PM version presented above, but with the stator height halved to 500 mm. Runs were carried out using a one-turn field current of 120 kA. This produces ~2 T in the air gap, so that the back EMF per section is exactly as for the PM machine, and the same currents produce ~ twice the shear stress and, therefore, the same total thrust. Since the inductance is halved by halving the conductor lengths, the track sectioning is reduced significantly. While it was initially thought that this shuttle might need to be superconducting, it turns out that because of the very short operational time a version using copper coils and carrying ultracapacitors is possible. An early design included 1200 kg of copper and 400 kg of ultracapacitors to provide the 6.6 MJ required to operate the coils for 5 s, the maximum launch time. The temperature rise of the copper in this 5 s is, however, ~14 °C, so that some form of rapid active cooling between firings would be necessary, for a noncryogenic solution.

One of most serious implications of increasing the air-gap flux density is, however, that the tooth iron fully saturates, so that the flux density in the slot and, thus, in the copper conductors, increases dramatically. This exposure to very high dB/dt's can result in massively increased eddy-current losses in the copper conductors. Fig. 18 shows the instantaneous power loss in the four conductors in a single slot when the shuttle passes over
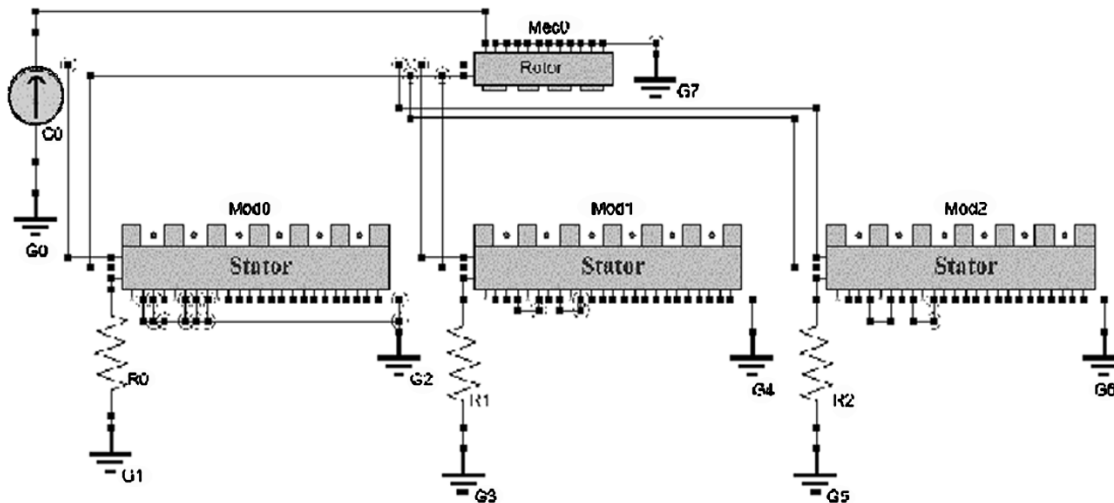
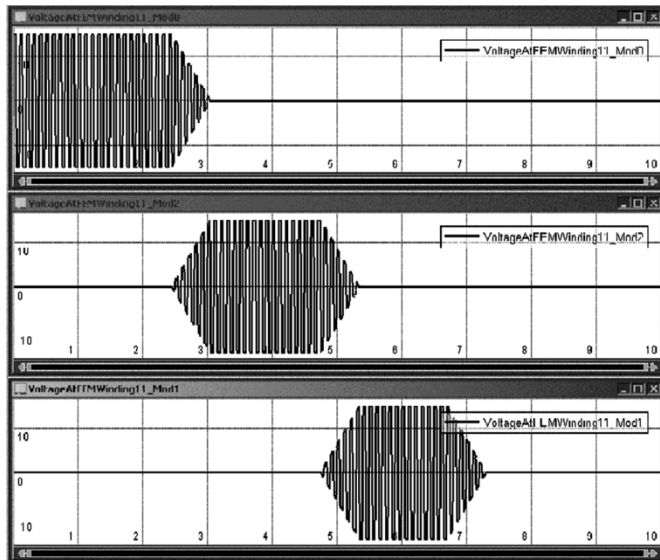Fig. 16.   VTB schematic for second simulation test.

Fig. 17.   Back EMF in the first three sections of the track, shuttle moving with constant velocity.
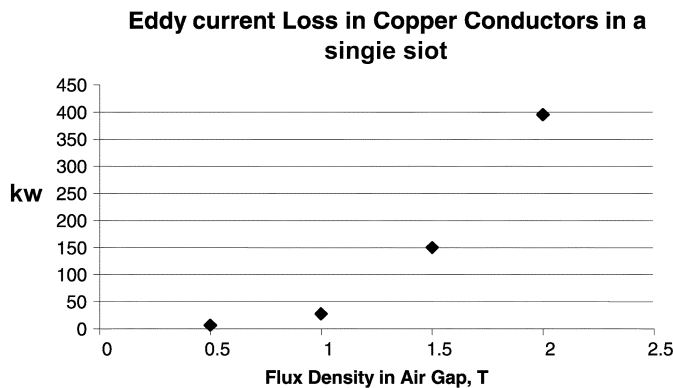

Fig. 18.   Instantaneous power loss in the four conductors in a single slot when the shuttle passes over them at 100 m/s, as a function of the air-gap flux density.

them at 100 m/s, as a function of the air-gap flux density. Clearly, while stranding will easily control the losses at $\sim$1 T with the PM machine, the wound-field machine will require much more aggressive attention to management of the likely eddy currents.

B. Induction Machine

Much time was spent attempting to design a competitive induction version, without great success. Without presenting these less effective designs in detail, what can be said is that for the same format as the PM machine, and using the same shuttle active material mass, i.e., $\sim$1200 kg of copper in sheets or coils ideally placed and carrying the current required to provide the same thrust, these coils would have a temperature rise of $\sim$8 °C per shot. Thus, either the shuttle needs to be cryogenic or some form of rapid active cooling will be necessary [17]. Then, we must arrange to induce that current with an additional magnetizing current in the stator. This has an immediate impact on the track sectioning, since the ΔI in the track sectioning equation (1) increases. Any design attempts to increase the flux in the air gap for the same current must increase the inductance by definition, and this again appears in (1). Once any section gets to be shorter than the shuttle itself, the quantum of power electronics switches (for driving, e.g., three sections simultaneously) begins to increase dramatically. Thus, the induction version will be expected to, for similar layouts, require active cooling and have a larger amount of power electronics. The induction motor system will be substantially more difficult to drive, since the magnetic circuit would be designed to maximize the flux in the air gap from current in the armature. Thus, the inductance of the armature winding will be higher, and the mutual inductance between phase windings will not be negligible.

VI. CONCLUSION

We conclude that the PM machine is a very good solution, being surprisingly small and simple, with a manageable but large power electronics switching system. The wound-field coil machine does not appear to provide sufficient advantage to justify the extra complexity, unless weight becomes a much more significant concern, but this configuration does have advantages in the power electronic system. The induction machine design will be very complex, requiring either cryogenics or active cooling, and the cost of the power electronics is liable to be substantially higher because of the higher inductances.

Fig. 19. Linear PM coaster launcher at Six Flags Holland. (Photograph reprinted with the permission of KumBak Coasters.)

A more global conclusion is that in relation to large machines, considering PM, induction machine, or wound-field types, the remarkable benefit of a PM design is twofold.

Firstly, it provides the ability to build structures with minimal inductance because of very large effective air gaps, resulting from the relative permeability of the NdFeB being ~ 1.

Secondly, a significant thermal penalty is avoided by using a PM rather than its equivalent model, a one-turn loop current. This substantial thermal penalty occurs in ambient-temperature wound-field machines as well as in induction machines.

VII. POST SCRIPT—DE-RISKING THE TECHNOLOGY

This work on a large-scale system with no physical demonstration has produced more than the usual number of concerns and doubts about the viability of, as one example, managing the very large forces of attraction. As evidence that these forces can be managed, and that such a large PM linear machine is indeed viable we cite a PM roller coaster launcher which was installed in 2000 at Six Flags in Holland [18]. Fig. 19 shows this system, in which a shuttle launches the roller coaster. The fin in the center below the shuttle provides reaction for the bearings which maintain the ~ 10-mm air gap either side of the double armature This machine is of the double inverted U layout, one on each side. It operates at a stress, estimated, using some given dimensions to be 80 kN/m^2, and has a thrust ~ 3 times that of the WWII Electropult. An installation of the same form has been in operation at Disney World in Orlando, FL, since July 1999, with continuous operation for up to 21 hours per day, a 48-s dispatch time, and operating 365 days per year. In the 40 months since the ride has been open to the public it has achieved a total number of launches in the region of 1.2 million. There have been no equipment failures during this time [19].

REFERENCES

[1] M. R. Doyle, D. J. Samuel, T. Conway, and R. R. Klimowski, "Electromagnetic aircraft launch system—EMALS," *IEEE Trans. Magn.*, vol. 31, no. 1, pp. 528–533, Jan. 1995.
[2] R. R. Bushway, "Electromagnetic aircraft launch system development considerations," *IEEE Trans. Magn.*, vol. 37, no. 1, pp. 52–54, Jan. 2001.
[3] D. Patterson, A. Monti, C. Brice, R. Dougal, R. Pettus, and T. Bertoncelli, "Design and simulation of an electromagnetic aircraft launch system," in *Proc. 17th Int. Conf. Magnetically Levitated Systems and Linear Drives, MAGLEV 2002*, Lausanne, Switzerland, Sep. 2002, CD-ROM.
[4] R. Dougal, T. Lovett, A. Monti, and E. Santi, " A multilanguage environment for interactive simulation and development controls for power electronics," in *Proc. IEEE PESC'01*, vol. 3, Vancouver, BC, Canada, Jun. 17–22, 2001, pp. 1725–1729.
[5] S. Yamamura, *Theory of Linear Induction Motors*. New York: Wiley, 1972.
[6] I. Boldea and S. A. Nasar, *Linear Motion Electromagnetic Systems*. New York: Wiley, 1985.
[7] ——, *Linear Electric Motors: Theory, Design, and Practical Applications*. Englewood Cliffs, NJ: Prentice-Hall, 1987.
[8] S. C. Ahn, J. H. Lee, and D. S. Hyun, "Dynamic characteristic analysis of LIM using coupled FEM and control algorithm," *IEEE Trans. Magn.*, vol. 36, no. 4, pp. 1876–1880, Jul. 2000.
[9] K. Davey, "Pulsed linear induction motors in Maglev applications," *IEEE Trans. Magn.*, vol. 36, no. 5, pp. 3703–3705, Sep. 2000.
[10] J. Faiz and H. Jafari, "Accurate modeling of single-sided linear induction motor considers end effect and equivalent thickness," *IEEE Trans. Magn.*, vol. 36, no. 5, pp. 3785–3790, Sep. 2000.
[11] "A wound rotor motor 1400 feet long," *Westinghouse Eng.*, pp. 160–161, Sep. 1946.
[12] T. J. E. Miller, *Brushless Permanent-Magnet and Reluctance Motor Drives*. London, U.K.: Oxford Univ. Press, 1989.
[13] J. E. Peoples, "EMALS aircraft structural fatigue life prediction," Naval Air Warfare Center Aircraft Division Lakehurst, Lakehurst, NJ, Rep. NAWCADLKE-DDR-05-PD-0008, Oct. 1992.
[14] K. Halbach, "Application of permanent magnets in accelerators and electron storage rings," *J. Apppl. Phys.*, vol. 57, pp. 2605–3608, 1985.
[15] C. Mi, G. R. Slemon, and R. Bonert, "Modeling of iron losses of surface-mounted permanent magnet synchronous motors," in *Conf. Rec. IEEE-IAS Annu. Meeting*, vol. 4, Chicago, IL, Oct. 2001, pp. 2585–2591.
[16] I. Boldea and S. A. Nasar, *Linear Electric Actuators and Generators*. Cambridge, U.K.: Cambridge Univ. Press, 1997.
[17] R. J. Elwell, R. W. Garman, and M. Doyle, "Thermal management techniques for an advanvced linear motor in an electric aircraft recovery system," *IEEE Trans. Magn.*, vol. 37, no. 1, pp. 476–479, Jan. 2001.
[18] D. Vatcher and J. Uittenbogaart, "Linear synchronous motor technology for launching roller coasters," in *Rec. Trends in Leisure and Entertainment Conf. Exhibition (TiLE)*, 2000, CD-ROM.
[19] D. Vatcher, private communication, Jan. 2003.

Dean Patterson (M'89–SM'94) received the B.E. (hons), M.E., Ph.D., and Dip. Ed. degrees from the University of Adelaide, Adelaide, Australia.

He recently completed 16 years at the Northern Territory University, Darwin, Australia, where he was Director of the Northern Territory Center for Energy Research and a lead participant in the Australia Cooperative Research Center for Renewable Energy. After three years as a Research Professor at the University of South Carolina, he is now a Visiting Professor at the University of Nebraska, Lincoln. His primary research focus is on very-high-efficiency electric machines and drives. He is the author of about 100 technical papers.

Prof. Patterson is a Fellow of the Institution of Engineers Australia. He has been very active in the IEEE Power Electronics Society.

Antonello Monti (M'94–SM'02) received the M.S. degree in electrical engineering and the Ph.D. degree from the Politecnico di Milano, Milan, Italy, in 1989 and 1994, respectively.

From 1990 to 1994, he was with the research laboratory of Ansaldo Industria, Milan, Italy, where he was responsible for the design of the digital control of a large power cycloconverter drive. From 1995 to 2000, he was an Assistant Professor in the Department of Electrical Engineering, Politecnico di Milano. Since August 2000, he has been an Associate Professor in the Department of Electrical Engineering, University of South Carolina, Columbia. He is the author or coauthor of more than 100 papers in the areas of power electronics and electrical drives.

Dr. Monti is a Member of the Computers in Power Electronics Committee of the IEEE Power Electronics Society and currently serves as its Chair. He also serves as an Associate Editor of the IEEE TRANSACTIONS ON AUTOMATION SCIENCE AND ENGINEERING.

Charles W. Brice (M'76–SM'83) received the B.E.E., M.S.E.E., and Ph.D. degrees from the Georgia Institute of Technology, Atlanta, in 1971, 1972, and 1977, respectively.

He has been a faculty member in the Department of Electrical Engineering, University of South Carolina, Columbia, since 1983. He was a faculty member in the Department of Electrical Engineering, Texas A&M University, College Station, from 1977 to 1983. He has research interests in power systems and machines and drives, and has been an Affiliate Professor for Project Lead the Way, a national consortium of pre-engineering programs since 2002.

Srinivas Dhulipala received the Bachelors degree in electronics and communication engineering from Nagarjuna University, Guntur, India, and the M.S.E.E. degree from the University of South Carolina, Columbia.

He is currently a Programmer–Analyst with Orion Systems Integrators, Edison, NJ. His research interests include work on electrical machines, and simulation of their characteristics and performance. He has worked on the analysis of linear machines using finite-element analysis (FEA). His simulation work used the Virtual Test Bed (VTB) platform.

Roger A. Dougal (S'74–M'78–SM'94) received the Ph.D. degree in electrical engineering from Texas Tech University, Lubbock, in 1983.

He then joined the faculty of the Department of Electrical Engineering, University of South Carolina, Columbia.

Dr. Dougal was the recipient of the Samuel Litman Distinguished Professor of Engineering Award and has been honored as a Carolina Research Professor.

Dilip Chandra Kovuri received the Bachelors degree in electronics and instrumentation engineering from Jawaharlal Nehru Technological University, Hyderabad, India, and the M.S.E.E. degree from the University of South Carolina, Columbia.

He is currently a System Administrator with BNP Paribas, New York, NY. His research interests are in the areas of electric machine design, electric machine characterization, and simulation using FEA and a range of simulation tools.

Robert O. Pettus received the B.S., M.S., and Ph.D. degrees in electrical engineering and mathematics from Auburn University, Auburn, AL, in 1963, 1965, and 1973, respectively.

He is currently a Professor in the Department of Electrical Engineering, University of South Carolina, Columbia. He originally worked in the fields of control, pulsed power, and communications. His work in computer architecture lead to the first documented microcomputer disk-based operating system and one of the first shared-memory multiprocessors.

Dr. Pettus is a Member of Eta Kappa Nu, Tau Beta Pi, and Sigma Xi.

Tiziana Bertoncelli graduated in electrical engineering and received the Ph.D. degree from the Politecnico di Milano, Milan, Italy, in 2000 and 2004, respectively.

She is currently an Assistant Researcher in the Dipartimento di Elettrotecnica, Politecnico di Milano. In the 2001, she was a Short Term Research Assistant in the Department of Electrical Engineering, University of South Carolina, Columbia, participating in the EMAL project. Her research interest are electromagnetic field analysis, design, and modeling of electrical machines, converters, and drive systems.